Low contact resistivity and strain in suspended multilayer graphene

Francisco P. Rouxinol, Rogério V. Gelamo, Renato G. Amici, Alfredo R. Vaz, and Stanislav A. Moshkalev

Citation: Appl. Phys. Lett. **97**, 253104 (2010); doi: 10.1063/1.3528354

View online: http://dx.doi.org/10.1063/1.3528354

View Table of Contents: http://apl.aip.org/resource/1/APPLAB/v97/i25

Published by the American Institute of Physics.

Low contact resistivity and strain in suspended multilayer graphene

Francisco P. Rouxinol,[a] Rogério V. Gelamo,[b] Renato G. Amici, Alfredo R. Vaz, and Stanislav A. Moshkalev
Center for Semiconductor Components, State University of Campinas, Campinas, Sao Paulo 13083-870, Brazil

(Received 27 August 2010; accepted 30 November 2010; published online 20 December 2010)

Method to prepare suspended multilayer graphene (MLG) flakes and to form highly conductive (contact resistivity of ~ 0.1 kΩ μm^2) and tight mechanical connection between MLG and metal electrodes is described. MLG flakes prepared from natural graphite were precisely deposited over tungsten electrodes using dielectrophoresis, followed by high-temperature thermal annealing in high-vacuum. Considerable strain induced in the suspended part of flakes was revealed by Raman imaging. © *2010 American Institute of Physics*. [doi:10.1063/1.3528354]

Methods of fabrication, modification, and characterization of graphene are currently under fast development.[1–4] Few layer graphene (FLG) properties depend significantly on the number of layers (N), usually approaching those of bulk graphite for relatively low N. Thermal conductivity of single layer graphene (SLG) is at least twice as high as for bulk graphite, but it falls to the level of bulk graphite already for $N=4$.[5] Raman scattering spectra (position and shape of G and 2D/G′ lines) were also shown to change strongly with the number of layers, becoming very close to those of graphite for $N\sim 10$.[6] However, multilayer graphene (MLG) ($N>5$) may have some advantages over SLG or FLG in a number of applications. In graphene based field effect transistors (FETs), higher "on" current is achievable for MLG-FET; furthermore it can have also better immunity to adverse substrate effects like charge impurities and oxide traps near the transistor channel as compared to SLG-FET.[7] Other applications may include gas sensors based on graphene flakes decorated by nanoparticles[8] and the use of MLG as templates to achieve ultimate resolution using focused ion beam processing.[9] In such applications, the enhanced mechanical and chemical stability of MLG is a critical advantage, together with much easier fabrication and further processing (e.g., decoration) as compared with FLG. Another advantage is associated with the possibility to obtain stable electrical contacts with electrodes using conventional thermal processing. In contrast, for a single layer the thermal processing can result in its destruction due to the formation of carbides or metal-carbon interdiffusion.[10,11]

In experiments with single and few-layer graphene, side-contact with metal is usually obtained (graphitic layers parallel to the metal surface). Due to the presence of impurities and roughness of the metal surface, the contact resistance (R_c) in this case can be quite high so that R_c frequently determines the total device resistance. A few studies so far reported measurements of metal-graphene contact resistance using four-probe or transfer length method.[12,13] Contact resistivity between Ni and MLG supported on SiO_2 (top contact) was measured to be ~ 1 kΩ μm^2, being only weakly dependent on N. Contact resistance (in this case, $R_c \sim 1$ kΩ) and resistivity are related as follows: $R_c=\rho_c/A$, where A is the contact area. The high residual contact resistance for the graphene based device (FET) was attributed to the fact that only the top layer (or two) effectively forms the contact due to low interlayer conductance. $R_c\sim 5$ kΩ was found for top Cr/Au contacts (contact area of a few μm^2), also nearly independent of N.[13] Lee *et al.*[14] studied suspended MLG flakes (~ 10 nm thick) deposited over Pd/Cr contacts, and similar values (a few kΩ μm^2) can be estimated for ρ_c. In all these works[12–14] no conventional thermal annealing was used, but annealing by passing a high current through the suspended MLG sample (inside a cryostat)[14] was found to improve R_c considerably.

The interaction of graphene with substrates can be used for tailoring of graphene properties, in particular, to induce strain.[15–17] Methods to induce tension or compression in graphene flakes include deposition of flakes on a flexible material followed by the substrate mechanical stretching or bending.[18] Strain in graphene can also be induced by thermal processing due to different thermal expansion coefficients for a substrate and graphene.[19,20]

Confocal Raman spectroscopy is a powerful tool for nondestructive measurements of graphene properties. G and 2D bands were shown to be highly sensitive to strain with negative and positive shifts observed for tension or compression, respectively. For FLG suspended over gaps fabricated in SiO_2, it was reported[19] that graphene compression due to thermal cycling reduces rapidly with the number of layers, practically disappearing for $N>10$, likely due to higher stiffness of thicker layers.

In our study, MLG flakes were prepared in solutions and deposited precisely over metal electrodes using ac dielectrophoresis (ac-DEP), and the effect of thermal annealing on the graphene properties and the graphene/metal contact was analyzed.

Suspensions of FLG/MLG in N,N-dimethylformamide were prepared by ultrasonication (10 min) and centrifugation (8000 rpm for 30 min) of natural graphite (Nacional de Grafite). Atomic force microscopy analysis shows that the flakes have thickness varying from 5 to 30 nm (with a smaller fraction of 1–2 nm thick flakes) and lateral dimensions between 1 and 10 μm. Using this suspension, graphene flakes were deposited over tungsten electrodes using ac-DEP. For short deposition times, individual flakes

[a]Electronic mail: rouxinol@ifi.unicamp.br.
[b]Present address: Instituto de Ciências Tecnológicas e Exatas, UFTM, Uberaba, Minas Gerais 38025-180, Brazil.

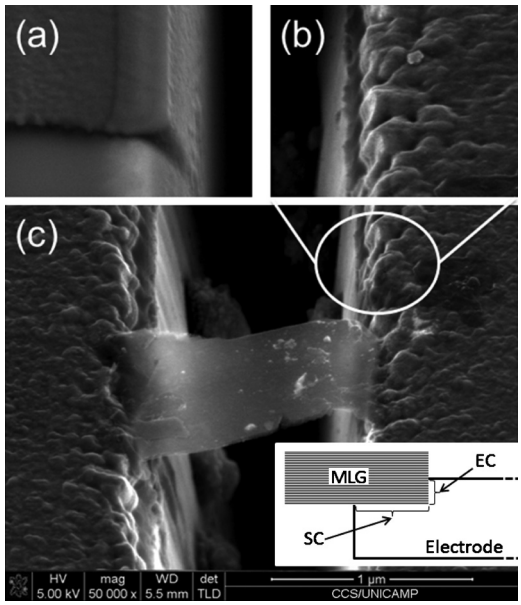

FIG. 1. SEM image of MLG flake between W electrodes after annealing (c). Fragments of electrode edges are shown before (a) and after (b) annealing. Inset in (c) shows the geometry of metal-MLG contact, SC, and EC—side- and end-contact areas.

were deposited between the electrodes with the yield up to 80%.

Tungsten electrodes (100 nm thick, 5 μm wide, deposited by sputtering) were fabricated over 400 nm thick insulating SiO_2 layers thermally grown on silicon. To deposit suspended graphene flakes, a focused ion beam (FIB) was employed for milling 5 μm deep and 1 μm wide cuts between metal electrodes. Tungsten was chosen as the electrode because its Fermi level is close to that of graphene (thus low contact resistance can be expected),[21] and thin W and C layers form alloys at relatively low temperatures (~800 °C).[22] To improve the contact between the MLG and the electrode, samples were thermally annealed in high-vacuum ($<5\times10^{-6}$ Torr) at 850 °C for 1 h.

An example of an individual 20 nm thick MLG flake deposited between electrodes is shown in Fig. 1. After annealing, the low-bias two terminal resistance was found to reduce from 0.7 MΩ to ~0.1 kΩ forming Ohmic contacts. For the flake in Fig. 1, the total resistance ($R_t=2R_c+R_g$) dropped to 70 Ω after thermal treatment. Considering the total side-contact area of ≤0.5 μm^2, contact resistivity is estimated to be $\rho_c\leq0.14$ kΩ μm^2 or even lower as the contribution of the flake resistance (R_g) must be subtracted. The R_g value is estimated as ~30 Ω, assuming graphite resistivity of 4×10^{-5} Ω cm and flake dimensions of 1.2, 0.8, and 0.02 μm for length, width, and thickness. The resulting contact resistivity (<0.1 kΩ μm^2) is ~10 times smaller than obtained in other studies without thermal annealing.[12–14] This improvement can be attributed to removal of impurities, formation of tungsten carbide in the interface area (WC is a good electrical conductor),[22] and the effectively increased physical contact area between the flake and the metal, though the end-contact area is estimated to be very small (~0.01 μm^2). The formation of such contact area and the formation of tungsten carbide in the metal-graphene interface were revealed by FIB cross-sectioning (not shown, see elsewhere[8]).

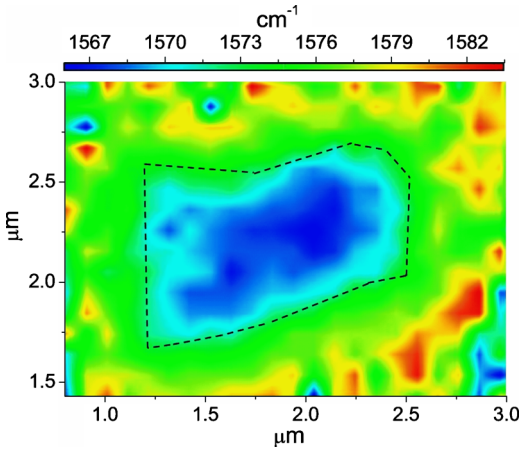

FIG. 2. (Color online) Raman image showing the position of the G peak within the flake; dashed line marks the flake physical borders (apparent image broadening is due to a finite laser beam radius of 0.3 μm).

Raman spectra and images of MLG were obtained at low intensity (0.1 mW) of the 632.8 nm laser to avoid possible sample heating. Figure 2 shows a Raman image of the G line peak position of the suspended flake after annealing. Figure 3 depicts the peak position and full-width at half maximum (FHWM) for the G line along the cross-sections in horizontal (a) and vertical (b) directions. The downshift of G lines to ~1567 cm^{-1} can be seen in the suspended part compared with ~1582 cm^{-1} at the flake borders. Note that before annealing, the G line position was unshifted (~1580–1582 cm^{-1}) along the entire flake surface. To improve the precision, spectra were also taken at some points within the flake with longer accumulation, and so measured G peak positions are shown in a histogram, Fig. 4(a). For the central part of a suspended area, the downshift is bigger (distribution centered at ~1567 cm^{-1}). The downshift is smaller for suspended edges, while for the area in contact with the electrode the distribution is centered near 1582 cm^{-1}, corresponding to usually reported values for MLG, see Fig. 4(b). Similar results were obtained for several suspended flakes, while no downshift was observed in flakes localized over silicon dioxide or metal surface after annealing.

Note that partial graphene oxidation can occur during thermal annealing due to residual oxygen; however, this

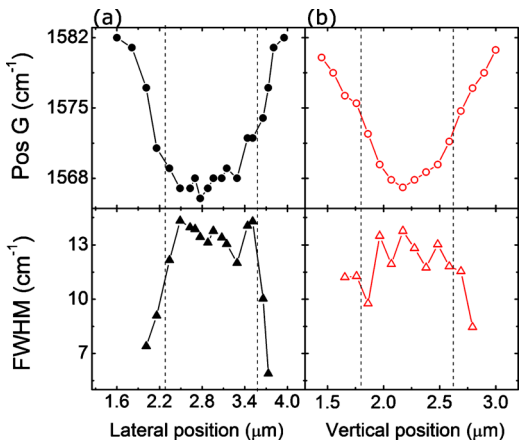

FIG. 3. (Color online) Variation of G line peak position (top) and FWHM (bottom) for cross-sections along the flake axis (a) and normally to it (b); dashed line marks the flake physical borders.

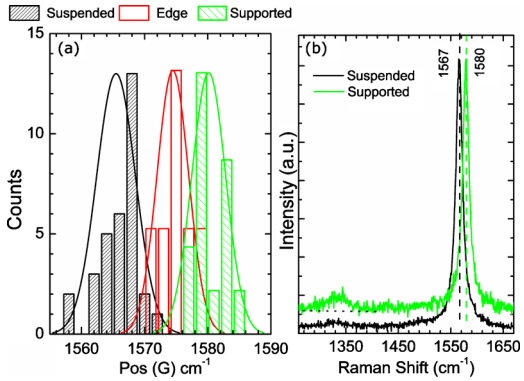

FIG. 4. (Color online) (a) Distribution of G line peak positions and Gaussian fitting for the central part of suspended area, edge area, and over electrodes. (b) Raman spectra for suspended area and over electrodes.

should result in upshift of the G line,[23] while downshift was observed in our case. Considerable G peak downshift (~ 10 cm^{-1}) was observed by Malard *et al.*[24] when graphene was heated to relatively high temperatures (250 °C). However, in our case heating by laser irradiation should be negligible at low power used in experiments (0.1 mW). Moreover, no peak downshift was observed in the suspended flakes before annealing. Special experiments using laser power up to 1 mW (see below) also did not show any measurable effect on the detected G line position. Careful analysis of the scanning electron microscopy (SEM) images reveals that the electrodes shrank after annealing [compare Figs. 1(a) and 1(b)] probably due to the metal compression and/or crystallization. In this process the gap between electrodes becomes slightly (0.1 μm) bigger. This process could cause considerable strain in the sample, resulting in the downshift observed in the suspended flake. Estimates of the stretching give $\sim 0.5\%$.[25] This result indicates that the formation of a strong mechanical connection between the flake and electrode material occurs *before* (and likely, at lower temperature) the electrode shrinkage.

Interestingly, measurements intentionally performed with elevated laser power (~ 1 mW) eventually resulted in disappearance of the G line downshift in a suspended area (G peak moved to 1582 cm^{-1} within the whole sample area), indicating irreversible damage of the flake, confirmed by SEM images and by an order of magnitude increase in the total resistance.

Finally, MLG was prepared from natural graphite and deposited over W electrodes using dielectrophoresis followed by thermal treatment. Formation of low-resistance Ohmic contacts ($\rho_c \sim 0.1$ kΩ μm^2) and tight mechanical connection between the metal and multilayer graphene in the interface area with a thickness of ~ 10 nm was observed.[8] The electrode shrinkage during the processing resulted in an increase of the interelectrode gaps and, in turn, in considerable strain induced in the suspended MLG as revealed by Raman imaging.

In the case of carbon nanotubes, reduction of metal-carbon contact resistivity due to gas pressure or thermal processing was studied in the nanotube based gas sensors.[26,27] Possible effects of strain induced by gas could also be considered for development of graphene based gas sensors.

This work was supported by the FAPESP, CNPq, and INCT NAMITEC.

[1] G. Tsoukleri, J. Parthenios, K. Papagelis, R. Jalil, A. C. Ferrari, A. K. Geim, K. S. Novoselov, and C. Galiotis, Small **5**, 2397 (2009).
[2] C. Soldano, A. Mahmood, and E. Dujardin, Carbon **48**, 2127 (2010).
[3] B. R. Burg, J. Schneider, S. Maurer, N. C. Schirmer, and D. Poulikakos, J. Appl. Phys. **107**, 034302 (2010).
[4] A. Vijayaraghavan, C. Sciascia, S. Dehm, A. Lombardo, A. Bonetti, A. C. Ferrari, and R. Krupke, ACS Nano **3**, 1729 (2009).
[5] S. Ghosh, W. Bao, D. L. Nika, S. Subrina, E. P. Pokatilov, C. N. Lau, and A. A. Balandin, Nature Mater. **9**, 555 (2010).
[6] A. Gupta, G. Chen, P. Joshi, S. Tadigadapa, and P. C. Eklund, Nano Lett. **6**, 2667 (2006).
[7] Y. Ouyang, H. Dai, and J. Guo, Nano Res. **3**, 8 (2010).
[8] F. P. Rouxinol, R. V. Gelamo, and S. A. Moshkalev (unpublished).
[9] J. Gierak, Semicond. Sci. Technol. **24**, 043001 (2009).
[10] M.-S. Wang, D. Golberg, and Y. Bando, Adv. Mater. (Weinheim, Ger.) **22**, 93 (2010).
[11] J. Lahiri and M. Batzill, Appl. Phys. Lett. **97**, 023102 (2010).
[12] A. Venugopal, L. Colombo, and E. M. Vogel, Appl. Phys. Lett. **96**, 013512 (2010).
[13] K. Nagashio, T. Nishimura, K. Kita, and A. Toriumi, Jpn. J. Appl. Phys. **49**, 051304 (2010).
[14] S. Lee, N. Wijesinghe, C. Diaz-Pinto, and H. Peng, Phys. Rev. B **82**, 045411 (2010).
[15] M. Bruna, A. Vaira, A. Battiato, E. Vittone, and S. Borini, Appl. Phys. Lett. **97**, 021911 (2010).
[16] C. Metzger, S. Remi, M. Liu, S. V. Kusminskiy, A. H. Castro Neto, A. K. Swan, and B. B. Goldberg, Nano Lett. **10**, 6 (2010).
[17] Y. Wang, Z. Ni, T. Yu, Z. X. Shen, H. Wang, Y. Wu, W. Chen, and A. T. S. Wee, J. Phys. Chem. C **112**, 10637 (2008).
[18] T. M. G. Mohiuddin, A. Lombardo, R. R. Nair, A. Bonetti, G. Savini, R. Jalil, N. Bonini, D. M. Basko, C. Galiotis, N. Marzari, K. S. Novoselov, A. K. Geim, and A. C. Ferrari, Phys. Rev. B **79**, 205433 (2009).
[19] C.-C. Chen, W. Bao, J. Theiss, C. Dames, C. N. Lau, and S. B. Cronin, Nano Lett. **9**, 4172 (2009).
[20] N. Levy, S. A. Burke, K. L. Meaker, M. Panlasigui, A. Zettl, F. Guinea, A. H. Castro Neto, and M. F. Crommie, Science **329**, 544 (2010).
[21] Q. Ngo, D. Petranovic, S. Krishnan, A. M. Cassell, Q. Ye, J. Li, M. Meyyappan, and C. Y. Yang, IEEE Trans. Nanotechnol. **3**, 311 (2004).
[22] E. Lassner and W. Schubert, *Tungsten: Properties, Chemistry, Technology of the Element, Alloys, and Chemical Compounds* (Plenum, New York, 1999).
[23] D. C. Kim, D. Y. Jeon, H. J. Chung, Y. S. Woo, J. K. Shin, and S. Seo, Nanotechnology **20**, 375703 (2009).
[24] L. M. Malard, R. L. Moreira, D. C. Elias, F. Plentz, E. S. Alves, and M. A. Pimenta, J. Phys.: Condens. Matter **22**, 334202 (2010).
[25] Z. H. Ni, T. Yu, Y. H. Lu, Y. Y. Wang, Y. P. Feng, and Z. X. Shen, ACS Nano **2**, 2301 (2008).
[26] C. Caillier, A. Ayari, V. Gouttenoire, A. SanMiguel, V. Jourdain, M. Picher, and J.-L. Sauvajol, Appl. Phys. Lett. **97**, 173111 (2010).
[27] R. V. Gelamo, F. P. Rouxinol, C. Verissimo, A. R. Vaz, M. A. Bica de Moraes, and S. A. Moshkalev, Chem. Phys. Lett. **482**, 302 (2009).